# Fracture Spacing and Orientation Estimation from Spectral Analyses of Azimuth Stacks

Mark Willis, Rama Rao, Daniel Burns, M. Nafi Toksoz
Earth Resources Laboratory
Dept. of Earth, Atmospheric and Planetary Sciences
Massachusetts Institute of Technology
Cambridge, MA  02139


Laura Vetri
Agip E.N.I., San Donato, Italy

**Abstract**

Discrete, vertically aligned fracture systems impart one or more notches in the spectral ratios of stacked reflected seismic traces.  This apparent attenuation is due to the azimuth dependant scattering introduced by the fractures. The most prominent notch is located at the frequency where the P wavelength is about twice the fracture spacing.    The frequency location of the notches can be used to determine the fracture spacings. Azimuth stacks with an orientation parallel to the fractures tend not show these spectral notches – allowing for another way to detect the fracture orientation.  An analysis of the vertical component of the 3D, ocean bottom cable seismic survey data from the Emilio field, offshore Italy, shows a prominent set of fractures with a spacing of about 30 to 40 meters with orientations that agree with previous studies.

## 1.      Introduction

There is a large body of the literature devoted to analyzing rocks with fracture sizes and spacings which are much less than one wavelength.  For these systems the rock will behave elastically as an effective anisotropic medium displaying the aggregate properties of a distribution of small fractures.  Lynn (2004a) gives a good summary of the differences between effective medium and discrete fractures.

Much of our recent work has been devoted to deriving fracture properties from vertical sets of discrete fractures which have dimensions and spacings on the order of the seismic wavelength (e.g. Willis et al, 2004a and 2004b). This study first derives spectral characteristics of azimuth stacks from modeled fractured systems and then applies these observations to seismic field data.

## 2.      Model Study – the Spectral Notch Method

We first analyze the surface seismic reflection traces created from a 3D, anisotropic finite difference algorithm.  The models consist of a sandwich of five layers, as shown in Figure 1.  The center layer is an isotropic reservoir containing discrete sets of gas-filled, vertical fractures represented by vertical planes made up of a single grid cell, with equivalent anisotropic medium properties determined using the method of Coates and Schoenberg (1995). We use models with different regular fracture spacings of 100m, 50m, 35m and one with a Gaussian distribution of fractures centered about 35m.

We create azimuth stacks of the shot records at 10 degree increments from normal to parallel to the fractures. As in our previous studies, we find that scattered energy from the fractures is reinforced on the stacks parallel to the fractures and is reduced in the direction normal to the fractures.  The left panel in Figure 2 shows the azimuth stacks for the 50m fracture spacing case.

From these azimuth stacks we create their associated transfer functions, as described by Willis et al. (2004).  Briefly, this process entails for each azimuth stack trace: 1) identifying a target depth range (the fractured layer) to

investigate 2) extracting a window of data containing reflections which are above this fractured layer (denoted as the input), 3) extracting a window of data below the fractured layer (denoted as the output) containing reflections which includes the scattered energy, 4) taking the autocorrelation of the extracted windows, 5) windowing the autocorrelations to focus on the source wavelet near zero lag and 6) computing the spectra ratio of the lower and upper windowed autocorrelations from the amplitude spectrum of the time domain transfer function (see Willis et al, 2004). The right panel in Figure 2 shows the time domain transfer functions for the 50m fracture case. The mean of corresponding amplitude spectra of the 50m case for azimuths within 40 degrees of normal to fracture strike is shown in Figure 3.
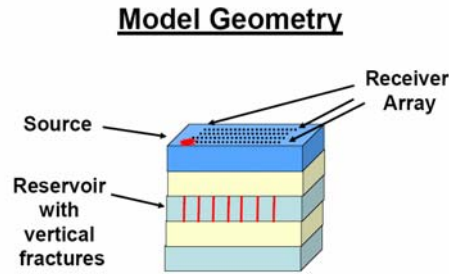


Figure 1. Model geometry – five layers with the center layer containing discrete vertical fractures.
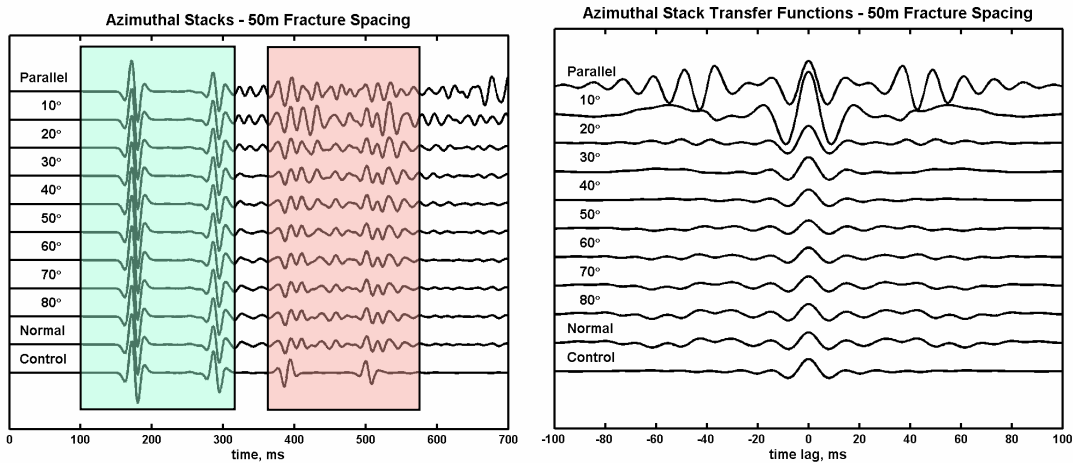


Figure 2. Left panel shows the azimuth stacks for the 50m regularly spaced fracture model. The two highlighted areas show the input (left most) and output (right most) windows used to compute the associated transfer functions in corresponding traces in the right panel.

On this display a deep notch in the spectrum at about 35 Hz can be seen. Since there is no attenuation in the model we would expect to see a nearly flat spectral ratio over the bandwidth of about 10 to 80 Hz. This is not the case. At this particular frequency energy in the propagating single happens to cancel out due to the time delay of a P wave traveling between two fractures and creating a null. The notch at about twice the fracture spacing is characteristic of all the models studied.

2

To further study this notch, we convert the frequency axis to a normalized scale, n, using the relationship n = Vp / (Frequency * Fracture Spacing) where Vp is the average P-wave velocity in the depth range of investigation.  Figure 4 shows the mean spectral ratios for all the models studied using this normalized scale.  Here we see the presence of a notch in each of the spectra at the normalized wavelength of about 1.5 to 2.  Higher order notches are present, but do not appear at the same place.
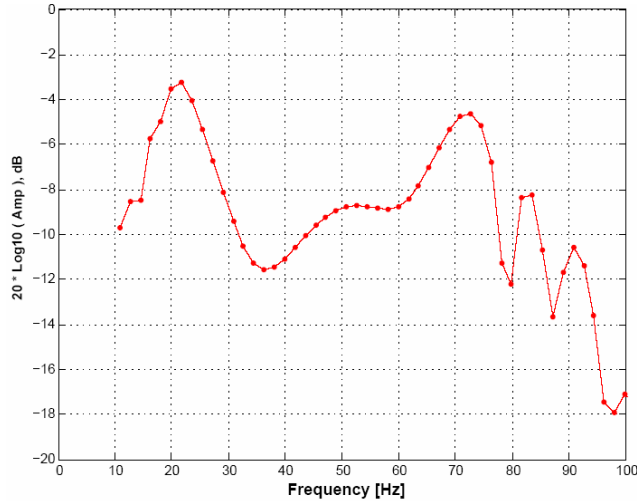


Figure 3. The mean of the spectral ratios for the 50m fracture case for azimuth stacks with orientations within 40 degrees of normal to the fracture strike. The vertical axis is in dB.
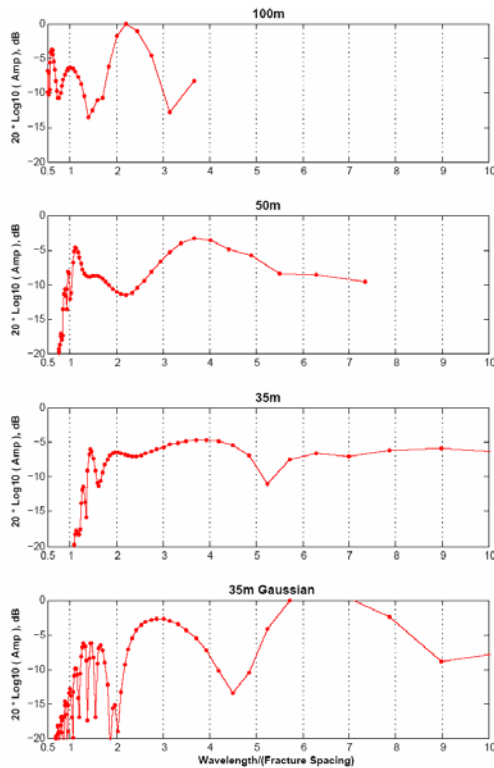


Figure 4. The spectral ratio plots for all four models.  Each spectrum is the mean of the spectra within 40 degrees of normal to the fracture strike.

3

In Figures 3 and 4 we have shown averages of the spectra using the azimuths within 40 degrees of the normal to the fracture strike. We excluded the spectral ratios in the remaining directions as the notch effect is reduced close to the fracture strike direction. This is due to the fractures acting like mechanical polarizers, channeling energy away from the normal direction, towards the parallel direction. Hence, in the parallel direction, there is in fact an amplification, or a peak in the spectral ratios. Thus, this azimuth sensitive behavior of the spectral ratios also provides fracture orientation. Lynn (2004b) has noted holes in the spectra shear components and attributed them to interference of backscattered energy.

## 3.    Emilio Field Data Study

In 2000, a 3D/4C seismic survey was collected over the Emilio Field, located in the central part of the Adriatic Sea, near the eastern coast of Italy. The reservoir unit is a fractured carbonate with two orthogonal fracture sets oriented ENE and NNW (Angerer et al, 2002). This field has been investigated using PP and PS wave anisotropy to identify fracture characteristics of the reservoir level (Minsley et al, 2004; Vetri et al, 2003; Gaiser et al, 2002).

We apply the spectral notch method, described above for the model data, to analyze the seismic data from the Emilio field. We selected the near to mid range offsets of the preprocessed PP data (Vetri et al, 2003) and created eighteen different azimuth stack volumes from East to West using 20 degree wide overlapping ranges. We created two superbins to collect the stacked traces around wells 4 and 8. The size of each superbin was 11x11 bins (125m x 250m). For each of the 18 azimuth stacks, the traces which fell within the two bins were collected. For each of these traces, a time window above, and another window below the reservoir were extracted and their autocorrelations computed.

While the time domain transfer function could be computed as an intermediate step using Weiner deconvolution, we directly computed the spectral ratios by spectral division of the fast Fourier transforms of the autocorrelations. We then averaged the spectral ratio values for all the traces with the same azimuth stack direction within the same superbin.

It should be noted that the signal-to-noise level in the data will dictate the viable frequency bandwidth, which in combination with P velocity of the layers under consideration defines an observable range of wavelengths and consequently fracture spacings for a given data set. For the current data set, observable fracture spacings are expected to be in the range 20 to 120 m.

Fig 5 shows the spectral ratio amplitudes as a function of azimuth and wavelength for well 4 (left) and 8 (right). The vertical axis shows each of the 18 azimuths from 0 degrees East, 90 degrees North and 170 degrees nearly West. Clearly evident on the figure is a significant azimuth variation of spectral ratio amplitudes. Further, prominent notches (blue) across a broad range of azimuths can be observed, particularly at fracture spacings of about 30m. From the model study, the notches are expected over a range of azimuths that are nearly perpendicular to the fracture direction. Additional features are the peaks (red) in both plots. Well 4 shows large amplitudes at about 70 and 120 degrees. Well 8 shows a band of large amplitudes at a range of azimuths from about 90 to 120 degrees. These larger amplitudes occur at spacings of 50 to 60 m, and are expected indicate directions that are close to the fracture strike directions. Thus the peaks and troughs are expected over perpendicular azimuths if only a single, equally spaced fracture set is present.
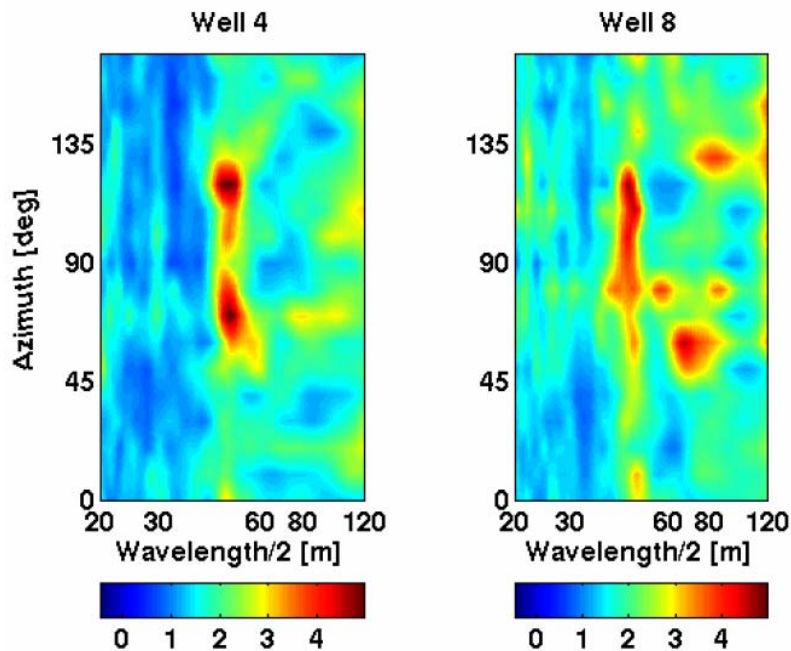
Figure 5. Spectral ratio functions for well 4 (left) and well 8 (right). The vertical axis is the direction of the azimuth stack where 0 degrees is East and 90 degrees it North. The horizontal axis is wavelength/2, which is interpreted as fracture spacing

Figure 6 shows the median spectral ratio, averaging over azimuths, for wells 4 (left) and 8 (right). A linear trend in the spectral ratio amplitude, attributable to attenuation (decreasing amplitude with increasing frequency), was removed. This curve amounts to a projection of the contours in Fig 5 along the x-axis.

Troughs are evident in both plots, consistent with discrete fractures spacing of about 30 to 40 m. A second, weaker trough around 60 to 80 m is discernable, corresponding to a twice fracture spacing, along with the peak around 50 to 60 m.
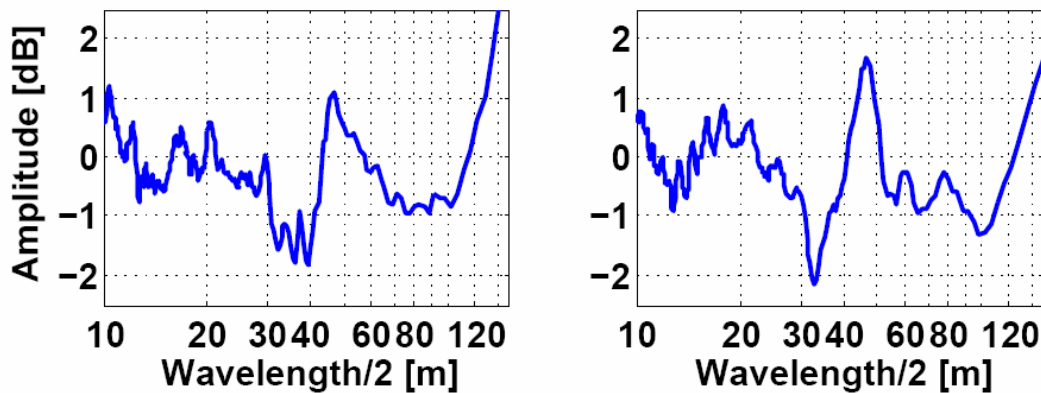


Figure 6. Averaged spectral ratios in the area around well 4 (left) and well 8 (right). The wavelength axis has been scaled by 2 so that fracture spacing may be read directly from the x-axis.

Some of these results can be validated with prior studies on this data. Figure 7 shows the borehole derived measurements for horizontal stress directions from Vetri et al. (2003). We've added the red arrow in the left rose

diagram to highlight the direction of maximum horizontal stress, since the breakouts appear in the minimum horizontal stress direction. Generally fractures tend to align subparallel to the maximum horizontal stress direction.

Estimates of the aggregated fracture orientations using these volumes from the analysis of scattering indices are shown as rose plots in Figure 8, modified from Willis et al. (2004). The rose plots, which estimate the distribution of fractures in the area around well 4 (left) and well 8 (right), agree with the ENE and NNW directions derived in the studies mentioned above and shown in Figure 7.
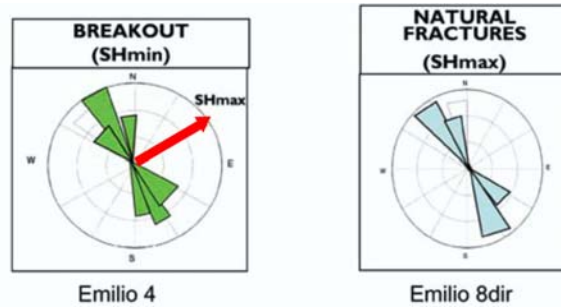


Figure 7. Borehole Measurements: Stress measurements from borehole break outs in well 4 (left) and from natural fractures observed in the borehole in well 8 (right) (modified from Vetri et al, 2003). Vertical fractures tend to be aligned with the maximum horizontal stress direction.
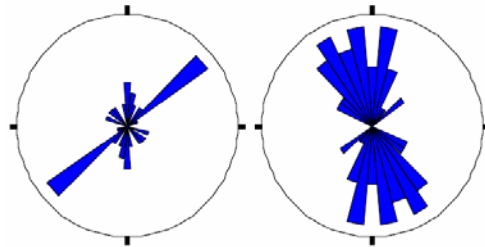


Figure 8. Scattering Index: Rose diagrams showing fracture orientations in the area surrounding well 4 (left) and well 8 (right) from an analysis of scattering indices (Willis et al, 2004).
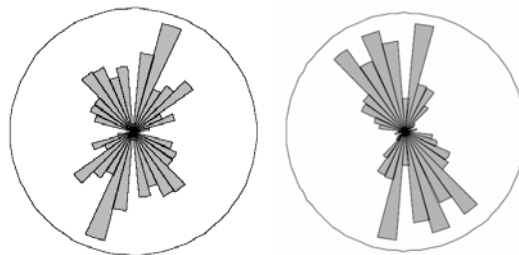


Figure 9. Spectral Notch Method: Rose diagrams showing fracture orientations using the method described in this paper, for the area surrounding well 4 (left) and well 8 (right).

For comparison, we derive a polar plot of the spectral ratio amplitudes for the bins corresponding to well 4 and 8 in Figure 9. Spectral ratio amplitudes are plotted versus angle, with the peak amplitudes identifying fracture directions. There is a reasonable consistency between the present results and prior work (Figs 7 and 8) in overall fracture directions. It should be noted that the three measures are at different scales: stress direction measurements in Fig 7 are essentially "point" measurements localized around a borehole, whereas the scattering index measures (Fig 8) are

for an area covering about 0.5km x 1km while the spectral notch method measures (Figure 9) are for an area of 0.125 km x .25 km.

# 4. Discussion and Conclusions

We have presented a spectral notch method for extracting fracture characteristics from surface seismic data. The data volume is subdivided into 18 azimuth stack volumes. Spectral ratios are computed using windows of seismic data above and below the target reservoir for all azimuth stacks. The azimuth variation of the spectral ratio values can be used to detect both the spacing and orientation of fractures in the reservoir. For azimuths about 40 degrees or closer to the direction normal to fracturing, we expect to see spectral ratio notches (or zeros) indicating the absorption of seismic energy. The notches are located at wavelengths which are about two times the fracture spacing. We expect that there is overall more energy, and thus more amplitude, in the spectral ratio for azimuths parallel to the fracture strike. These trends are clearly evident on the finite difference derived model data.

We applied the spectral notch method to the PP data derived from the 3D/4C Emilio field data. We observed significant variation with azimuth of the spectral ratios over the entire survey. We frequently observed notches corresponding to fracture spacings of 30 to 40 meters over the survey. Fracture orientations were also extracted using this approach and they agreed with prior studies, including borehole breakout and natural fracture analyses. They also agreed with estimates of seismically derived fracture orientations from scattering indices. These three results are consistent with each other even though they were derived from measurements averaged at three different scales – point (well based), 0.04 km2 (spectral ratio notches), and 2.5 km2 (scattering index).

# 5. Acknowledgements

# References

Angerer, E, Horne, S, Gaiser, J., Walters, R., Bagala, S., 2002, Characterization of dipping fractures using Ps mode-converted data, SEG Expanded Abstracts.

Coates, R. T., and Schoenberg, M., 1995, Finite-difference modeling of faults and fractures, Geophysics, 60, n5.

Gaiser, J., Loinger, E., Lynn, H, and Vetri, L, 2002, Birefringence analysis at the Emilio field for fracture characterization, First Break v 20, 505-514.

Lynn H., 2004a, The winds of change: Anisotropic rocks – their preferred direction of fluid flow and their associated seismic signatures – Part 1, The Leading Edge, Nov.

Lynn, H., 2004b, The winds of change: anisotropic rocks – their preferred direction of fluid flow and their associated seismic signatures, Part II, The Leading Edge, Dec.

Lynn, H., Simon, K. M., and Bates, C. R., 1996, Correlation between P-wave AVOA and S-wave traveltime anisotropy in a naturally fractured gas reservoir, The Leading Edge, v 15, 931-935.

Minsley, B., Willis, M., Krasovec, M., Burns, D., and Toksoz, M.N., 2004, Investigation of a fractured reservoir using P-wave AVOA analysis: a case study of the Emilio Field with support from synthetic examples, SEG Expanded Abstr. 23, 248.

Vetri, L., Loinger, E. Gaiser, J. Grandi, A., Lynn, H, 2003, 3D/4C Emilio: Azimuth processing and anisotropy analysis in a fractured carbonate reservoir, The Leading Edge, 675-679.

Willis, M.E. and Rao, R., 2005, Attenuation losses induced by discrete vertically aligned fractures, EAGE Expanded Abstr., Madrid.

Willis, M.E., Pearce, F, Burns, D.R, Byun, J. and Minsley, B, 2004a, Reservoir fracture orientation and density from reflected and scattered seismic energy, EAGE meeting Paris.

Willis, M.E., Rao, R., Burns, D., Byun, J, and Vetri, L, 2004b, Spatial orientation and distribution of reservoir fractures from scattered seismic energy, 74th SEG Expanded Abstr., Denver.